Manipulating optical rotation in extraordinary transmission by hybrid plasmonic excitations

Tao Li,[1,a)] Hui Liu,[1] Shu-Ming Wang,[1] Xiao-Gang Yin,[1] Fu-Ming Wang,[1] Shi-Ning Zhu,[1,a)] and Xiang Zhang[2]
[1]*National Laboratory of Solid State Microstructures, Nanjing University, Nanjing 210093, People's Republic of China*
[2]*5130 Etcheverry Hall, Nanoscale Science and Engineering Center, University of California, Berkeley, California 94720-1740, USA*

(Received 27 April 2008; accepted 23 June 2008; published online 15 July 2008)

Polarized optical transmission properties through the L-shaped holes array in silver film was investigated at near infrared wavelength. Besides the enhanced transmission due to the combined plasmonic excitations, strong optical rotation was definitely observed at specific polarized incidences. After elaborate analyses, two eigenmodes were clearly characterized as the results of the hybrid localized plasmon resonances. Any polarization states from the incidences will degenerate into these two eigenstates after transmissions, suggesting a practical method to manipulate the polarization of light. Our result demonstrates the giant rotation rate achieved by the nanothin sample, indicating potential applications in the micro-optical devices. © *2008 American Institute of Physics*. [DOI: 10.1063/1.2958214]

Since the pioneering work of Ebbesen *et al.* of extraordinary optical transmission (EOT),[1] the interaction between the light and the surface plasmon excitation in metallic micro/nanostructures acquires a growing attention of research, not only for the fascinating fundamental physics but also for its wide potential applications in photonic devices, sensors, and so on.[2–4] Tremendous studies have been carried out to expose the relationship between the surface plasmon polartion (SPP) and EOT phenomenon.[5–8] Nevertheless, besides the enhanced transmission intensity, polarization state is another important characteristic in optics. Researchers have found the strong polarization dependence related to the localized surface plasmon (LSP) excitation arising from the holes shape resonance.[9–11] However, most of these LSP modes are relative simplex, in which the enhanced transmissions are always limited in one polarization state lacking variability and controllability. From this point, it is difficult to effectively change the polarization states and control the optical rotation in those systems.

In this letter, we report an experimental realization of manipulating the polarization state of the light and achieving giant optical rotation in near infrared wavelength by a nanometer thickness structure. Actually, using chiral structures or metamaterials to manipulate the optical polarization has arrested considerable interest in the nearest years.[12–19] Unfortunately, these designs usually demand complex nanostructures, which are relative difficulty to fabricate for the response in optical region. However, for the proposed structure, only simple L-shaped holes are introduced in the single metallic film, which are much easier in fabrication even in the nanoscale. Moreover, it combines the advantageous of the SPP enhanced transmission and LSP assisted optical rotation, suggesting potential applications in micro-optical controller or devices.

The tabulated samples were prepared by sputtering silver onto a quartz substrate and followed with the etching of focused-ion beam (FIB) (Strata FIB 201, FEI Company, 30 keV Ga ions). Upper-left inset in Fig. 1 is the designed one unit cell of this L-shaped hole array, where P, a, and b represent the period, arm length, and arm width, respectively. The fabricated sample contains $81\times81=6561$ L-shaped holes in total, covering an area about 49×49 μm^2. The lower right inset is a typical FIB image of the sample from the top view, where the structural parameters are $P=600$ nm, $a=300$ nm, $b=150$ nm, and the silver film thickness is about 80 nm. Optical measurement is schematically designed, as shown in Fig. 1. In our homebuilt optical setting, a polarized light from an illumination of a 50 W halogen lamp (wavelength 400–1800 nm) incidents normally onto the tabulated sample with the polarization angle θ_1 after

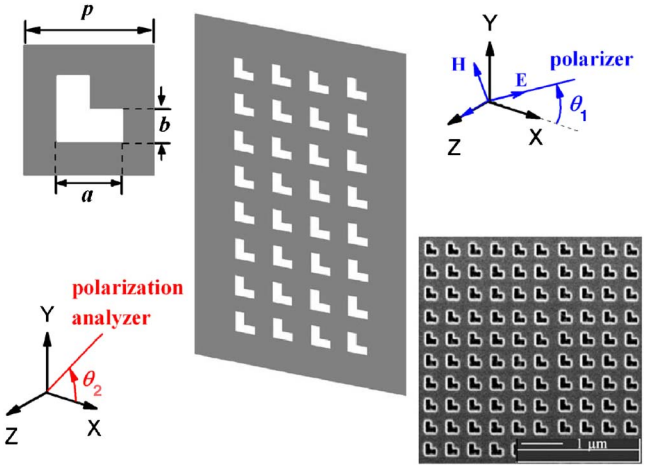

FIG. 1. (Color online) Schematic of experimental setup of the polarized transmission analyses for any given polarizer incidence after the L-shaped hole array sample. Upper-left inset is the designed one unit cell of this L-shaped hole array, and lower-right inset is a typical FIB image of the sample from the top view, where the structural parameters are $a=300$ nm, $b=150$ nm, and $P=600$ nm.

[a)]Authors to whom correspondence should be addressed. Electronic addresses: taoli@nju.edu.cn and zhusn@nju.edu.cn.

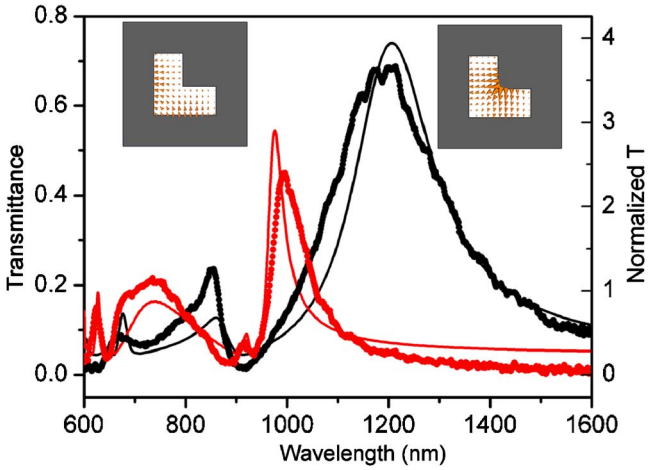

FIG. 2. (Color online) Measured (symbols) and calculated (lines) transmission spectra for the polarization of $\theta_1=-45°$ (red) and $\theta_1=45°$ (blue) cases, and value of right label is the normalized transmittance with respect to the hole occupation ratio. Insets are the simulated electric field distributions inside the hole of two eigenstates. The right one is for $|\alpha\rangle$ (1200 nm at $\theta_1=45°$) and the left one is for $|\beta\rangle$ (990 nm at $\theta_1=-45°$).

a Glan–Thomson prism. After the polarization check by another Glan–Thomson prism, the nearly zero-order transmitted light is collected by an optical spectrum analyzer (ANDO AQ-6315A) via a fiber coupler. By tuning the second prism, we can easily obtain the transmittance of the light through the sample in any preferred polarization state, defined by an angle of θ_2. Here, an angle difference between the incidence and polarization checking is defined as δ.

Considering the geometric symmetry, incidences with polarization along and transverse to the symmetric axis ($\theta_1=45°$ and $\theta_1=-45°$) are firstly investigated without the polarization checking. Symbols in Fig. 2 are the measured transmission spectra for these two polarization cases. It is clearly manifested that two distinct states are observed with strong transmission peaks at 1200 and 990 nm with respect to incidence at $\theta_1=45°$ and $\theta_1=-45°$, respectively. Subsequently, the second prism is added behind the sample to check the polarization state of the transmitted light. As estimated, the transmission spectra seldom changes as polarization analyzer is set as same as the polarizer ($\theta_2=\theta_1$), and the spectra shape keep unchanged only with weaker intensities for the cases of analyzer violating from the polarizer ($\theta_2\neq\theta_1$). This definitely indicates that the polarization states are maintained after the transmission for these two polarized incidences. Thus, these two particular states can be regarded as two eigenmodes $|\alpha\rangle$ and $|\beta\rangle$. Noticeably, if we normalize the transmission intensities to the occupation ration of these holes, the maximum transmittances reach about as large as 3.7 and 2.4 for the $|\alpha\rangle$ and $|\beta\rangle$ states, respectively, exhibiting the enhanced transmission property.

To examine the exact mode characters, we perform numerical analysis based on a commercial software package (CST Microwave Studio), by which the field distributions and transmission properties can be conveniently simulated.[15] Here, the dielectric constant of silver is defined by Drude mode with $\omega_p=1.37\times10^{16}$ s^{-1} and $\gamma=8.5\times10^{13}$ s^{-1},[20,21] and that of quartz substrate is set as 2.16 referring to the experimental parameter. Polarization states after the transmission can be calculated from the detected field amplitudes and phases in two orthogonal directions (along x and y axes). The

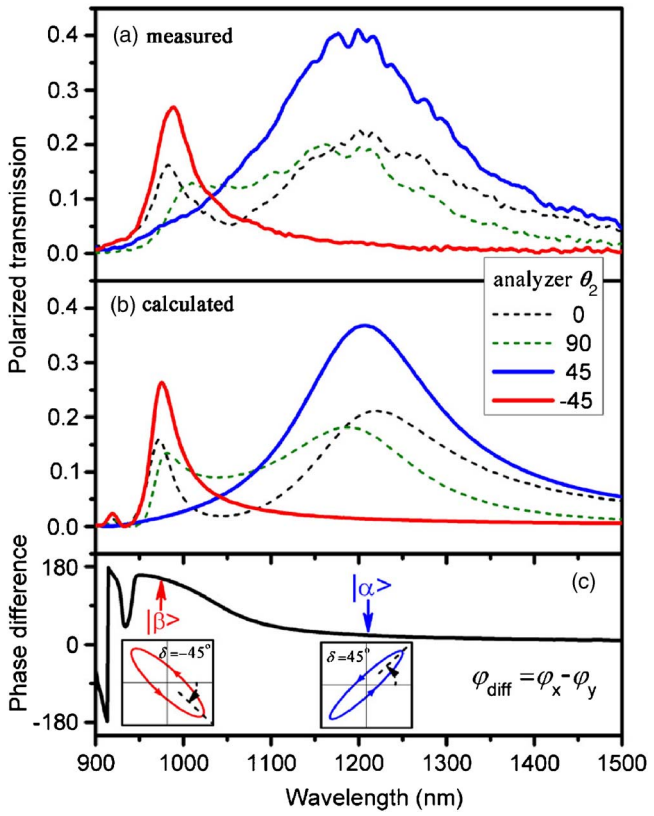

FIG. 3. (Color online) (a) Measured and (b) calculated transmission spectra with the polarization analyzer set at $\theta_2=0°$, 45°, 90°, and −45°, in the case of the polarizer of $\theta_1=0°$. (c) Phase difference between the detected phases in x and y directions ($\varphi_{diff}=\varphi_x-\varphi_y$) as the function of the wavelength, where insets are the calculated polarization states of the transmitted light at two eigenfrequencies.

solid curves in Fig. 2 are the calculated transmission spectra of these two specific incidences, which agree well with the measured ones. The two insets in Fig. 2 are the corresponding E field distributions inside the L-shaped holes corresponding to the $|\alpha\rangle$ and $|\beta\rangle$ states, respectively, both exhibiting strong resonance features but with orthogonal polarizations. Actually, these two modes can be considered as the hybrid LSP modes of two rectangular holes with two kinds of coupling, in-phase and antiphase, with respect to the symmetric axis of L-shaped holes. Considering the positions of two peaks with respect to the reciprocal dominated SPP excitation position, the stronger transmittance of state $|\alpha\rangle$ compared with $|\beta\rangle$ further verifies more enhanced transmission due to more contribution from the LSP resonance than the SPP excitations.

Afterwards, we test the cases with the incident polarization away from the two eigenstates. Evidently, the largest violation is the polarizer at $\theta_1=0°$ or 90°, and these two cases are identical due to the geometric symmetry. So we will mainly investigate the case of $\theta_1=0°$ in the following. Figure 3(a) shows the measured transmission spectra with the polarization analyzer set at $\theta_2=0°$, 45°, 90°, and −45°. Remarkable differences in the spectra are observed. From the figure, analyzed results with polarization of $\theta_2=45°$ and −45° are very similar to cases of $|\alpha\rangle$ and $|\beta\rangle$ eigenstates, only with a little weakening in the peak intensities. Otherwise, weaker and hybrid features are manifested in the spectra in the other cases—the original polarization state ($\theta_2=0°$) and its orthogonal state ($\theta_2=90°$). This means, in a common

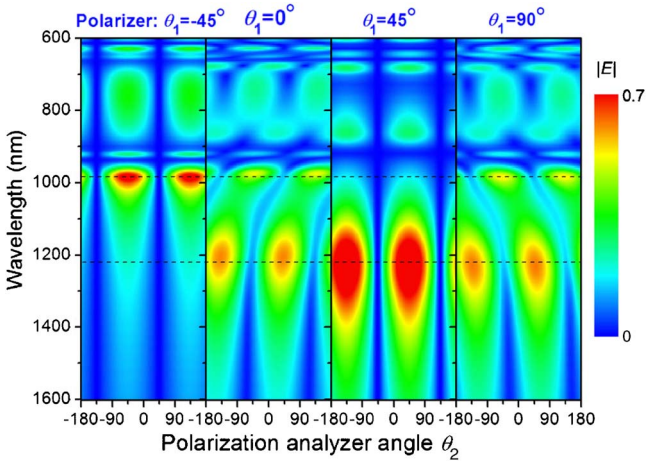

FIG. 4. (Color online) Simulated $|E|$ maps of transmitted light with respect to polarization analyzer θ_2 ranges from −180° to 180°, in four polarized incidence cases (θ_1=−45°, 0°, 45°, and 90°).

sense, that the polarization state with the strongest energy transmission is changed, or the optical polarization is rotated. Specifically, light polarization transmitted through the sample is rotated to $|\alpha\rangle$ state at 1200 nm and to $|\beta\rangle$ state at 990 nm with the rotation angle of about 45° and −45°, respectively.

Correspondingly, detailed numerical studies are performed on this incidence state as $\theta_1=0°$. Transmitted field amplitudes E_x (E_y) and phases φ_x (φ_y) in x (y) direction are conveniently obtained by the simulations. With these data, we can easily calculate the intensity of transmitted electric field in any polarization state (θ_2) as

$$|E_{\theta 2}| = [(E_x \cos\varphi_x \cos\theta_2 + E_y \cos\varphi_y \sin\theta_2)^2 + (E_x \sin\varphi_x \cos\theta_2 + E_y \sin\varphi_y \sin\theta_2)^2]^{1/2}. \quad (1)$$

To compare with the experimental data, we calculate the polarized transmission spectra via $T=|E_{\theta 2}|^2/|E_0|^2$, where the θ_2 is set as 0°, 90°, 45°, and −45° accordingly. Figure 3(b) shows the calculated results, which exhibits extremely good accordance with the measured ones. Afterwards, the phase difference ($\varphi_{\text{diff}}=\varphi_x-\varphi_y$) between the x and y directions is also depicted in Fig. 3(c). From the well known equation[22]

$$\left(\frac{E_x}{|E_x|}\right)^2 + \left(\frac{E_y}{|E_y|}\right)^2 - \frac{E_x E_y}{|E_x||E_y|}\cos\varphi_{\text{diff}} = \sin^2\varphi_{\text{diff}}, \quad (2)$$

we can obtain the transmitted polarization state in any wavelength. It is evident that in $|\alpha\rangle$ state, the phase difference is about 20° resulting in a counterclockwise elliptic polarization with the major axis rotation of δ=45°, while in $|\beta\rangle$ state the phase difference is about 150° leading to another elliptic polarization with a rotation of δ=−45°, as shown in the insets of Fig. 3(c). From the phase difference profile, we also conclude that linear polarization states can be obtained at about 915 nm or much larger wavelength. However, in those regions, the transmission is very weak and worthy of little consideration.

Moreover, we analyze other incidence cases by simulations as well as the case of $\theta_1=0°$. Figure 4 is an overview map of transmitted electric field distributions with respect to different polarization analyzer (θ_2 ranges from −180° to 180°) in four polarized incidences (θ_1=−45°, 0°, 45°, and 90°). Two eigenmodes are distinguishably exhibited separately in θ_1=−45° and 45° cases with strongest E field at about 990 and 1220 nm correspondingly. While, apparent distortions of the field map are observed in $\theta_1=0°$ and 90° cases with the strongest field distorting from the incidence polarization states, indicating obvious optical rotations. So far, it gives a clear description optical rotation effect by this silver film drilled with L-shaped holes array.

In conclusion, we have designed and fabricated the structure with L-shaped nanoholes array in a thin silver film for the light polarization manipulation. Optical transmission properties together with the polarization states are experimentally investigated in detail. It is definitely illustrated that enhanced transmissions with optical rotations are obtained at two particular wavelengths, which are considered as two eigenmodes attributing to the hybrid localized plasmon resonances. About 45° polarization rotation is achieved with relative strong transmissions for the specific polarized incidences ($\theta_1=0°$ or 90°) at the eigenfrequencies. It is a giant optical rotation rate considering our sample is only 80 nm thick. Such a design suggests the potential applications in the micro-optical devices.

This work is supported by the National Natural Science Foundation of China (Grant Nos. 10704036, 10604029, and 10534020), the State Key Program for Basic Research of China under Grant No. 2006CB921804.

[1] T. W. Ebbesen, H. J. Lezec, H. F. Ghaemi, T. Thio, and P. A. Wolff, Nature (London) **391**, 667 (1998).
[2] H. Diltbacher, J. R. Krenn, G. Schider, A. Leitner, and F. R. Aussenegg, Appl. Phys. Lett. **81**, 1762 (2002).
[3] B. Rothenhausler and W. Knoll, Nature (London) **332**, 615 (1998).
[4] M. M. Baksh, M. Jaros, and J. T. Groves, Nature (London) **427**, 139 (2004).
[5] H. F. Ghaemi, T. Thio, D. E. Grupp, T. W. Ebbesen, and H. J. Lezec, Phys. Rev. B **58**, 6779 (1998).
[6] L. Martin-Moreno, F. J. Garcia-Vidal, H. J. Lezec, K. M. Pellerin, T. Thio, J. B. Pendry, and T. W. Ebbesen, Phys. Rev. Lett. **86**, 1114 (2001).
[7] W. L. Barnes, W. A. Murray, J. Dintinger, E. Devanx, and T. W. Ebbesen, Phys. Rev. Lett. **92**, 107401 (2004).
[8] P. Lalanne and J. P. Hugonin, Nat. Phys. **2**, 551 (2006).
[9] K. J. K. Koerkamp, S. Enoch, F. B. Segerink, N. F. van Hulst, and L. Kuipers, Phys. Rev. Lett. **92**, 183901 (2004).
[10] M. Beruete, M. Navarro-Cia, M. Sorolla, and I. Campillo, Opt. Express **15**, 8125 (2007).
[11] M. Beruete, M. Navarro-Cia, M. Sorolla, and I. Campillo, J. Appl. Phys. **103**, 053102 (2008).
[12] A. V. Rogacheva, V. A. Fedotov, A. S. Schwanecke, and N. I. Zheludev, Phys. Rev. Lett. **97**, 177401 (2006).
[13] M. Theil, M. Decker, M. Deubel, M. Wegener, S. Linden, and G. von Fremann, Adv. Mater. (Weinheim, Ger.) **19**, 207 (2007).
[14] M. Decker, M. W. Klein, M. Wegener, and S. Linden, Opt. Lett. **32**, 856 (2007).
[15] H. Liu, D. A. Genov, D. M. Wu, Y. M. Liu, Z. W. Liu, C. Sun, S. N. Zhu, and X. Zhang, Phys. Rev. B **76**, 073101 (2007).
[16] J. M. Hao, Y. Yuan, L. X. Ran, T. Jiang, J. A. Kong, C. T. Chan, and L. Zhou, Phys. Rev. Lett. **99**, 063908 (2007).
[17] E. Plum, V. A. Fedotov, A. S. Schwanecke, N. I. Zheludev, and Y. Chen, Appl. Phys. Lett. **90**, 223113 (2007).
[18] T. Q. Li, H. Liu, T. Li, S. M. Wang, F. M. Wang, R. X. Wu, P. Chen, S. N. Zhu, and X. Zhang, Appl. Phys. Lett. **92**, 131111 (2008).
[19] J. M. Hao and L. Zhou, Phys. Rev. B **77**, 094201 (2008).
[20] T. Li, J. Q. Li, F. M. Wang, Q. J. Wang, H. Liu, S. N. Zhu, and Y. Y. Zhu, Appl. Phys. Lett. **90**, 251112 (2007).
[21] T. Li, S. M. Wang, H. Liu, J. Q. Li, F. M. Wang, S. N. Zhu, and X. Zhang, J. Appl. Phys. **103**, 023104 (2008).
[22] J. D. Jackson, *Classical Electrodynamics* (Wiley, New York, 1999).